

# Sub-Millimeter-Scale Measurement of Local Convective Heat Transfer Coefficient Exceeding $100 \text{ W}/(\text{m}^2 \cdot \text{K})$ Using an Optical Pump-Probe Method

Tao Chen<sup>1</sup>, Puqing Jiang<sup>1,\*</sup>

<sup>1</sup>*School of Power and Energy Engineering, Huazhong University of Science and Technology, Wuhan, Hubei 430074, China*

**ABSTRACT:** Conventional methods for measuring the local convective heat transfer coefficient ( $h_c$ ) often rely on simplifying assumptions that can compromise accuracy. Pump-probe methods like time-domain thermoreflectance (TDTR) avoid these assumptions but are limited to  $h_c$  values larger than  $30 \text{ kW}/(\text{m}^2 \cdot \text{K})$  due to modulation frequency constraints. This study introduces an optical-based Square-Pulsed Source (SPS) method, expanding the frequency range from 10 MHz to 1 Hz, enabling measurements of  $h_c$  values above  $100 \text{ W}/(\text{m}^2 \cdot \text{K})$  with uncertainties under 10%. The efficacy of the SPS method is demonstrated through measurements of local  $h_c$  in an impingement heat transfer process with a single round gas jet. The local Nusselt number distribution is compared with existing literature correlations, offering insights into convective heat transfer phenomena. This study presents a novel tool for measuring local intrinsic convective heat transfer coefficients, enhancing the understanding of local convective heat transfer.

**Keywords:** Square-Pulsed Source (SPS) method; local convective heat transfer coefficient; impingement heat transfer; sub-millimeter resolution; pump-probe method

## 1. Introduction

As technology advances, the need for precise thermal management becomes increasingly critical, necessitating measurements of the local convective heat transfer coefficient ( $h_c$ ) with sub-millimeter-scale spatial resolution. One primary motivation is the rising cooling demand for modern electronic devices, where effective cooling solutions, such as microchannel heat sinks and microjet impingement, require high-

resolution  $h_c$  measurements for optimized design and performance [1]. Beyond electronics, accurate local  $h_c$  measurement is crucial in various industrial and scientific applications, such as cooling turbine blades in aerospace engineering [2], targeted thermal therapies in biomedical fields [3], and controlling material properties in advanced manufacturing [4]. Precise  $h_c$  measurement not only optimizes convective heat transfer processes and improves energy efficiency but also validates computational models, thereby advancing thermal science and technology .

Currently, the common method for determining local  $h_c$  is the direct method [5]. This approach involves applying a uniform heat flux to the wall surface and simultaneously measuring the local wall temperature and the fluid temperature to calculate  $h_c$  based on Newton's law of cooling. However, this method is susceptible to inaccuracies due to several factors. For instance, inevitable heat loss makes it challenging to accurately determine the heat flux transferred to the fluid. Additionally, inserting temperature sensors can disturb the flow field, particularly in confined spaces such as microchannels. When the wall temperature is not uniform, heat conduction occurs within the wall, a phenomenon typically ignored by assuming one-dimensional heat transfer in the analysis. Moreover, large variations in fluid temperature necessitate the use of the "film temperature" concept. Furthermore, the direct method encounters difficulties in measuring high  $h_c$  values because high  $h_c$  values require a large heat flux to maintain the necessary temperature difference, exacerbating the heat loss effect.

Alternative methods, such as the mass transfer analogy method [6, 7] and laser interferometry [8, 9], can measure local  $h_c$  in specific situations but also have limitations. The heat-mass analogy method struggles to ensure identical boundary conditions, such as the constant heat flux boundary condition in heat transfer problems, which is challenging to impose in mass transfer problems. The zero wall velocity condition may also be violated due to the presence of a normal velocity component near the wall caused by mass transfer. The laser interferometry method, on the other hand, faces difficulties when measuring in confined spaces.

Optical pump-probe methods offer innovative approaches for measuring local  $h_c$ . Techniques such as time-domain thermoreflectance (TDTR) and frequency-domain

thermoreflectance (FDTR) have been used to measure local convective heat transfer [10-14]. In these methods, a transparent wall coated with a thin metal film undergoes the convective heat transfer process. A modulated pump laser passes through the transparent wall and focuses on the metal film to apply a localized heat flux, while a probe laser detects the temperature response of the metal film at the same spot. By establishing a heat transfer model and fitting the measurement signal optimally, the local  $h_c$  from the wall surface to the fluid can be extracted. However, TDTR's modulation frequency is limited to 0.1 to 10 MHz, restricting measurements to  $h_c$  values larger than 30 kW/(m<sup>2</sup>·K) [14].

Recently, a new pump-probe method called Square-Pulsed Source (SPS) has been developed to measure the thermal properties of bulk and thin-film materials [15, 16]. This method allows for the observation of signal variation in the time domain and a wide range of variable modulation frequencies from 1 Hz to 10 MHz. This capability enables the measurement of in-plane thermal diffusivity and cross-plane thermal effusivity across a broad range of materials with thermal conductivities from 0.2 to 2000 W/(m·K) [15], as well as the determination of the full anisotropic thermal conductivity tensor [16]. In this work, we demonstrate that the SPS method can also measure local  $h_c$  values greater than 100 W/(m<sup>2</sup>·K) with a typical uncertainty of less than 10%.

This paper details the basic principles of the SPS method for measuring local  $h_c$ , applies it to measure the local convective heat transfer coefficient of an air impinging jet, and compares the results with empirical correlations from the literature. Our findings indicate that the SPS method is a valuable new tool for local convective heat transfer measurement, offering significant advantages in improving measurement accuracy and expanding the measurement range.

## **2. Experimental Method**

### *2.1 Square-Pulsed Source Method*

The principle of the SPS method has been described elsewhere [15, 16]. Briefly,

the SPS method uses a square-wave-modulated pump laser to heat the sample, and a probe beam to detect the temperature response of the sample's surface. The reflected probe beam is collected by a balanced amplified detector, the electrical output of which is then transmitted to a periodic waveform analyzer (PWA) for rapid acquisition of the temperature amplitude change signal over one heating cycle. The measured signals are normalized for both the amplitude and the time, and then best fitted by a thermal model to extract the thermal properties of the sample.

A schematic diagram of the SPS system applied for local  $h_c$  measurements is shown in Figure 1. The measured sample is a transparent and lowly conductive substrate coated with a thin metal transducer film, with the surface of the metal film undergoing convective heat transfer processes. Here, we choose a 1-mm-thick PMMA plate as the substrate, and a 100-nm-thick Al film as the metal transducer. PMMA has a thermal conductivity of  $0.19 \text{ W}/(\text{m} \cdot \text{K})$  and a heat capacity of  $1.644 \text{ MJ}/(\text{m}^3 \cdot \text{K})$  [17] at room temperature, favorable for measuring  $h_c$ . The Al film has a high thermorefectance coefficient at our probe wavelength of 785 nm and serves as a good transducer for thermorefectance measurements.

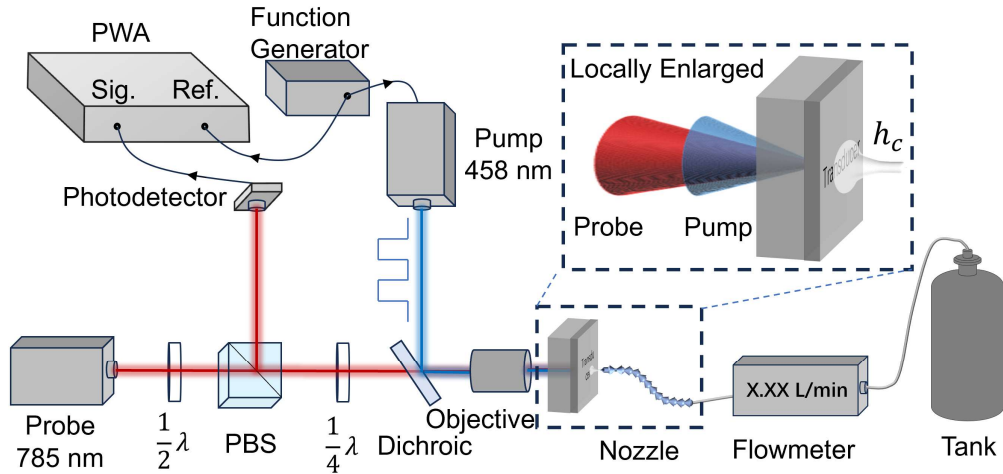


**Fig. 1.** Schematic diagram of the experimental system for measuring the local convective heat transfer coefficient of an air jet using the Square-Pulsed Source (SPS) method.

## 2.2 Heat Transfer Model

The role of the heat transfer model is to simulate and optimally fit the measurement

signal to extract the thermal properties of the material. The heat transfer model is based on the heat diffusion equation in cylindrical coordinates:

$$C \frac{\partial T}{\partial t} = \frac{k_r}{r} \frac{\partial}{\partial r} \left( r \frac{\partial T}{\partial r} \right) + k_z \frac{\partial^2 T}{\partial z^2} \quad (1)$$

where  $k_r$  and  $k_z$  are the thermal conductivities of the wall material in the radial and axial directions, respectively, and  $C$  is the volumetric heat capacity of the wall material.

A thin metal film is deposited on the surface of the transparent substrate. Heating and temperature detection occur at the interface between the metal film and the substrate, with convective heat transfer happening on the surface of the metal film, which is a third-type boundary condition. Through a series of derivations, the Green's function for the temperature response in the frequency domain can be obtained as:

$$\hat{G}(\rho, \omega) = \frac{\theta_0}{Q_0} = \frac{1}{\frac{\gamma_2}{\frac{\gamma_2}{G} + 1} + \frac{\gamma_1^2 \cdot \tanh\left(\frac{L}{k_{z1}} \gamma_1\right) + h_c \gamma_1}{h_c \cdot \tanh\left(\frac{L}{k_{z1}} \gamma_1\right) + \gamma_1}} \quad (2)$$

where  $Q_0$  is the applied heat flux density,  $\theta_0$  is the detected temperature response,  $\gamma = \sqrt{(4\pi^2 \rho^2 k_r + i\omega C)k_z}$ ,  $\rho$  is the Hankel transform variable,  $\omega$  is the angular frequency,  $L$  represents the thickness of the metal film,  $G$  is the interfacial thermal conductance between the metal film and the substrate, and  $h_c$  is the convective heat transfer coefficient on the surface of the metal film. The subscripts 1 and 2 represent the metal film and the transparent substrate, respectively.

In SPS measurements, the heat flux density applied by the pump laser is spatially distributed as a Gaussian with a radius of  $r_1$  and temporally as a square wave function with a frequency of  $f_0$ . After performing the Hankel transform and Fourier transform, the expression for  $Q_0$  is:

$$Q_0(\rho, \omega) = A_0 \exp\left(-\frac{\pi^2 \rho^2 r_1^2}{2}\right) \left(\frac{\delta(\omega)}{2} + \frac{1}{\pi} \sum_{n=1}^{\infty} i \frac{(\delta(\omega + (2n-1)\omega_0) - \delta(\omega - (2n-1)\omega_0))}{2n-1}\right) \quad (3)$$

where  $A_0$  is the power of the pump laser absorbed by the sample, and  $\omega_0 = 2\pi f_0$ .

Substituting the expression for  $Q_0$  into Eq. (2) gives the temperature response  $\theta_0$  in the frequency domain. Applying the inverse Hankel and Fourier transforms to  $\theta_0$  yields the temperature expression  $\Delta T_t$  in the time domain. The spatially weighted average of  $\Delta T_t$  with a probe laser radius of  $r_2$  distributed as a Gaussian is then

calculated, resulting in the signal variation over time detected by the photodetector as:

$$\begin{aligned} \Delta T(t) = & \frac{A_0}{2} \int_{-\infty}^{\infty} \hat{G}(\rho, 0) \exp(-\pi^2 \rho^2 r_0^2) 2\pi\rho d\rho \\ & - 2A_0 \operatorname{Re} \left( \sum_{n=1}^{\infty} \frac{i}{(2n-1)\pi} e^{i(2n-1)\omega_0 t} \right) \int_{-\infty}^{\infty} \hat{G}(\rho, (2n-1)\omega_0) \exp(-\pi^2 \rho^2 r_0^2) 2\pi\rho d\rho \end{aligned} \quad (4)$$

where  $r_0 = \sqrt{\frac{r_1^2 + r_2^2}{2}}$ .

The solution for  $\Delta T(t)$  must be obtained numerically. By normalizing this numerical solution, it can be compared with the experimentally measured signal to extract the parameters of interest.

The heat transfer model involves nine parameters: modulation frequency  $f_0$ , spot radius  $r_0$ , thermal conductivity  $k_m$ , specific heat capacity  $C_m$ , and thickness  $h_m$  of the metal film; thermal conductivity  $k$  and specific heat capacity  $C$  of the transparent wall material; interfacial thermal conductance  $G$  between the metal film and the wall; and convective heat transfer coefficient  $h_c$ . Among these,  $f_0$  is a set value, input parameters  $r_0$ ,  $k_m$ , and  $h_m$  can be independently measured or calibrated through measurements of standard samples, and  $C_m$  can be obtained from the literature. The values of  $k$  and  $C$  for the transparent wall material can be sourced from the literature or independently measured using the SPS method. At low frequencies, the measurement signal is typically insensitive to  $G$ , leaving  $h_c$  as the only parameter to be fitted.

### 2.3 Sensitivity Analysis and the Principle of Measuring Convective Heat Transfer Coefficients

The effect of various parameters on the normalized amplitude signal is described by the sensitivity coefficient  $S_\xi$ :

$$S_\xi = \frac{\partial A_{\text{norm}}/A_{\text{norm}}}{\partial \xi/\xi} \quad (5)$$

where  $A_{\text{norm}}$  is the normalized amplitude signal, and  $\xi$  represents any parameter to be analyzed. According to this definition,  $S_\xi$  indicates that a 1% change in parameter  $\xi$  will cause a  $S_\xi$  % change in the signal  $A_{\text{norm}}$ . Before conducting actual measurements, a sensitivity analysis of the signal should be performed to determine

whether the SPS method can accurately measure thermal property parameters and to select measurement conditions for optimal results.

Through in-depth sensitivity analysis, we found that to precisely measure convective heat transfer coefficients as low as  $100 \text{ W}/(\text{m}^2\cdot\text{K})$ , low thermal conductivity materials should be used as the transparent substrate, and a square wave modulation frequency below 1 Hz should be employed. Mathematically, such a setup reduces the proportion of the term  $\frac{\gamma_2}{\gamma_2+1}$  in the denominator of the temperature response function (Eq. (2)), thereby significantly enhancing the signal sensitivity to  $h_c$ . When the measurement target is a higher convective heat transfer coefficient, these conditions can be appropriately relaxed. For example, if the target convective heat transfer coefficient is on the order of  $1 \text{ kW}/(\text{m}^2\cdot\text{K})$ , the modulation frequency can be adjusted to 10 Hz. This finding provides crucial guidance for accurately measuring convective heat transfer coefficients.

### **3. Measurement Results and Discussion of Air Impinging Jet**

This study confirms the feasibility and accuracy of the SPS method for measuring the local convective heat transfer coefficient  $h_c$  by measuring the local convective heat transfer coefficient of an air impinging jet. Impinging jet cooling is considered an efficient means to enhance the convective heat transfer rate between a fluid and a surface. This mechanism relies on the jet directly impinging on the solid surface, where strong turbulent mixing and boundary layer renewal at the impact surface significantly increase the local heat transfer coefficient [18]. However, the local convective heat transfer intensity of an impinging jet is not uniform. Fine measurement and in-depth understanding of these thermal dynamics are crucial for optimizing impingement cooling systems, as they allow engineers to predict the positions with the best cooling effect and design nozzle arrangements and operating conditions to maximize heat transfer at the desired locations.

In the experiments presented in this paper, the wall material used was optical-grade acrylic (PMMA), with a nominal thickness of 100 nm aluminum film deposited on its

surface by magnetron sputtering as the temperature sensing layer. The actual thickness of the aluminum film was measured to be 93 nm using a step profiler. This film thickness value can be further verified through SPS measurements on standard samples: a standard fused quartz sample was placed alongside the PMMA sample during aluminum film deposition, and it can be assumed that the mass and thickness of the aluminum film deposited on both samples are the same. Using a  $37.5 \mu\text{m}$  spot radius and a 2 MHz modulation frequency, SPS measurements were conducted on the fused quartz sample. The measured signal was only sensitive to the parameter  $\sqrt{k_z C} / (h_m C_m)$ . Since the physical properties  $\sqrt{k_z C}$  of fused quartz and the heat capacity  $C_m$  of aluminum film are known, this measurement can determine the aluminum film thickness  $h_m$ . The result matched the step profiler measurement, with a smaller error of about 3%. The thermal conductivity  $k_m$  of the aluminum film can be determined from its electrical resistivity using the Wiedemann-Franz law, which is  $45 \pm 5 \text{ W}/(\text{m} \cdot \text{K})$ , and the resistivity can be measured using the van der Pauw method.

Compressed air at room temperature was ejected from a nozzle with a diameter  $D = 2 \text{ mm}$  at a flow rate of  $Q = 5 \text{ L}/\text{min}$  towards the surface of the metal film at a distance  $H = 15 \text{ mm}$  from the nozzle. This operating condition corresponds to a Reynolds number ( $Re$ ) of  $Re = uD/\nu = 3520$ . SPS measurements were conducted using a  $29 \mu\text{m}$  laser spot radius and a 1 Hz modulation frequency. The signals measured at the center of the impinging jet region for a complete heating cycle is shown in Fig. 2(a), where the symbols represent the measured signals and the curve represents the simulated signal of the heat transfer model at optimal fit. The heating and cooling segments of the temperature response signals are plotted on logarithmic coordinates in Fig. 2(b) and (c), respectively, for a more detailed examination of the fit quality between the simulated and measured signals. The simulated signals with  $\pm 30\%$  variation in the best-fit  $h_c$  are shown as dashed lines in Fig. 2(b) and (c), demonstrating the high sensitivity of the measured signal to  $h_c$ . The sensitivity coefficients of the measured signals to all the parameters in the heat transfer system are plotted in Fig. 2(d) and (e). The sensitivity curves show that, for both the heating and cooling segments of the

temperature response, the signals are mainly sensitive to the combined parameter  $k_r/(Cr_0^2)$  and the convective heat transfer coefficient  $h_c$ . Here,  $k_r/C$  is the in-plane thermal diffusivity of PMMA and can be sourced from the literature, with an uncertainty of around 3%. The laser spot radius  $r_0$  can be calibrated through SPS measurements using the same configurations on the same sample but without air impingement flow. After determining these parameters, the convective heat transfer coefficient  $h_c$  can be determined by best-fitting this set of signals, resulting in  $h_c = 700 \text{ W}/(\text{m}^2 \cdot \text{K})$  with an estimated error of 7%.

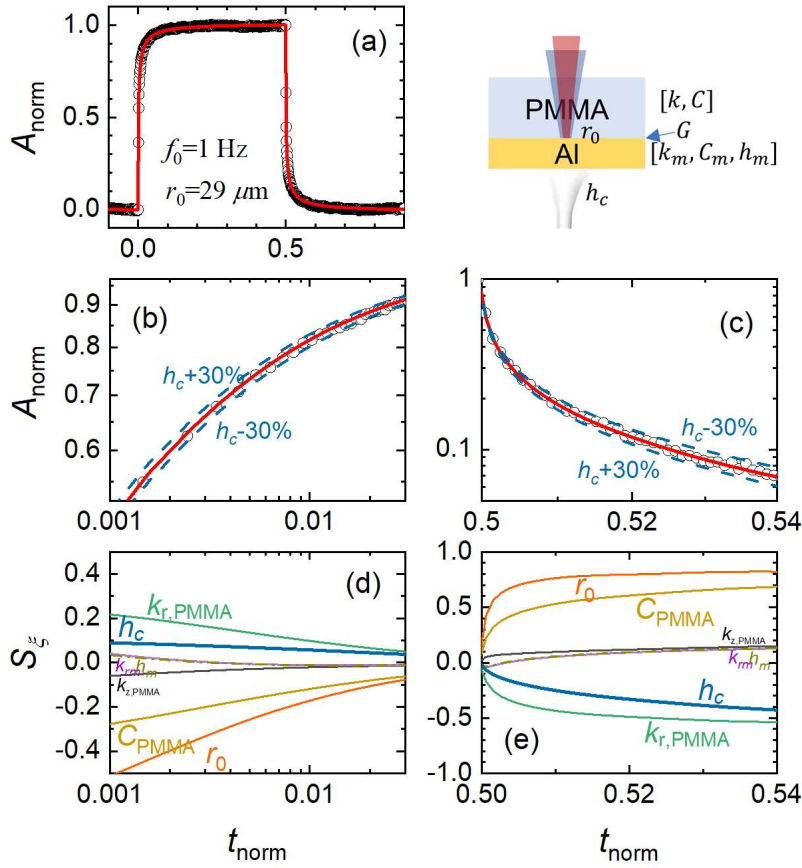


**Fig. 2.** SPS experimental signals and sensitivity curves at the center of the convective heat transfer region of the air impinging jet with a modulation frequency of 1 Hz and a spot radius of  $29 \mu\text{m}$ .

Figure 3 shows the variation of the local Nusselt number ( $Nu$ ) with the dimensionless radial distance ( $r/D$ ) with the nozzle positioned at different distances from the wall surface ( $H/D$ ), revealing the complexity of heat transfer in the impinging jet convective heat transfer system. Here,  $Nu$  is defined as  $Nu = h_c D/k_f$ , with  $h_c$

being the local convective heat transfer coefficient,  $D$  being the nozzle diameter, and  $k_f$  being the thermal conductivity of dry air and is taken as  $0.0257 \text{ W}/(\text{m} \cdot \text{K})$  at room temperature.

Initially,  $Nu$  reaches a peak in the acceleration stagnation region due to the high-speed impingement of the jet and intense turbulence, resulting in extremely high local heat transfer efficiency. As  $r/D$  increases,  $Nu$  first decreases, indicating that the jet slows down due to increased contact area with the surface, reducing turbulence and jet kinetic energy. Then, a second peak appears in the transition region, possibly due to interactions between the jet and the surrounding fluid, such as the formation of vortices or reattachment of the fluid to the surface, causing a sudden increase in turbulence intensity. As the jet continues to spread outward, its momentum further weakens, eventually becoming a standard wall jet, at which point the heat transfer capability decreases, leading to a subsequent decline in  $Nu$  values.

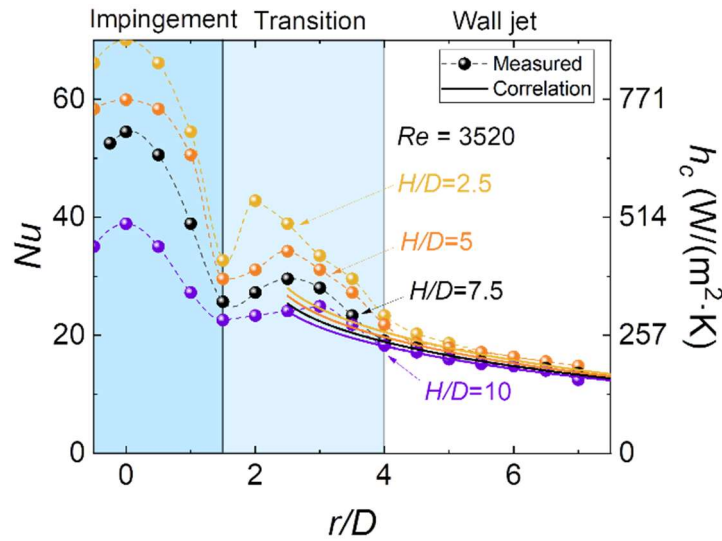


**Fig. 3.** Variation of SPS experimental  $Nu$  measurements (symbols connected by dashed lines) with  $r/D$  at different distances between the nozzle and the wall surface, and empirical values from the literature (solid lines).

There has been extensive research on impinging jet convective heat transfer in the literature. Martin conducted a comprehensive review of impinging jet convective heat transfer for single and array nozzles [19]. Most of the measurement results within the deceleration wall jet region are highly consistent in the literature, but there are

significant differences in the acceleration stagnation region and the transition region, which may be due to different turbulence levels at the nozzle outlet. Therefore, the literature only provides an empirical correlation for the average Nusselt number ( $\overline{Nu}$ ) in the deceleration wall jet region [19]:

$$\overline{Nu} \equiv \bar{h}_c D / k_f = 2 \frac{D}{r} \frac{1-1.1D/r}{1+0.1(H/D-6)D/r} Re^{1/2} (1 + 0.005 Re^{0.55})^{0.5} Pr^{0.42} \quad (6)$$

where  $\bar{h}_c$  is the average convective heat transfer coefficient from the jet center to a disk of radius  $r$ ,  $D$  is the nozzle diameter, and  $k_f$  is the thermal conductivity of the fluid. The applicable range of Eq. (6) is:  $2.5 \leq r/D \leq 7.5$ ,  $2 \leq H/D \leq 12$ , and  $2 \times 10^3 \leq Re \leq 4 \times 10^5$ .

Based on the relationship between the average Nusselt number  $\overline{Nu}$  and the local Nusselt number  $Nu$ , i.e.,  $\overline{Nu} = \frac{1}{\pi r^2} \int_0^r Nu(x) \cdot 2\pi x \cdot dx$ , the expression for the local Nusselt number  $Nu$  can be derived as:

$$Nu(r) = \frac{1}{2\pi} \frac{d}{dr} (\overline{Nu} \cdot \pi r^2) \quad (7)$$

Equation (7) is plotted as solid curves in Fig. 3 and compared with the experimental measurements in this study. It can be seen that in the wall jet region ( $r/D \geq 4$ ), the two agree perfectly, whereas there are no effective empirical correlations in the acceleration stagnation region and the transition region.

#### 4. Conclusion

This study proposes an innovative method for measuring the local intrinsic convective heat transfer coefficient—the Square-Pulsed Source (SPS) method. By using square wave modulated laser heating on the convective wall surface and another laser to detect wall temperature changes, this method offers high efficiency and flexibility. The SPS method can achieve spatial resolution smaller than 0.1 mm and measure local convective heat transfer coefficients exceeding 100 W/(m<sup>2</sup>·K) with a measurement error of less than 10%. In the air impinging jet experiment, the SPS method demonstrated excellent measurement performance, significantly enhancing the accuracy and range of local convective heat transfer measurements. This method provides a new tool for measuring local convective heat transfer, aiding in the further

understanding and optimization of convective heat transfer processes.

## **DATA AVAILABILITY**

The data that support the findings of this study are available from the corresponding author upon reasonable request.

## **DECLARATION OF COMPETING INTEREST**

The authors have no known competing interest to declare.

## **ACKNOWLEDGMENT**

This work is supported by the National Natural Science Foundation of China (NSFC) through Grant No. 52376058.

## **REFERENCES**

- [1] D.-Y. Lee, K. Vafai, Comparative analysis of jet impingement and microchannel cooling for high heat flux applications, *Int. J. Heat Mass Transfer*, 42 (1999) 1555-1568.
- [2] J.E. Town, D.L. Straub, J.B. Black, K.A. Thole, T.I.-P. Shih, State-of-the-Art Cooling Technology for a Turbine Rotor Blade, *Journal of Turbomachinery*, DOI (2017).
- [3] X. Li, J.F. Lovell, J. Yoon, X. Chen, Clinical development and potential of photothermal and photodynamic therapies for cancer, *Nature Reviews Clinical Oncology*, DOI (2020) 1-18.
- [4] Y. Li, W. Li, T. Han, X. Zheng, J. Li, B. Li, S. Fan, C.-w. Qiu, Transforming heat transfer with thermal metamaterials and devices, *Nature Reviews Materials*, 6 (2020) 488 - 507.
- [5] T.A. Moreira, A.R.A. Colmanetti, C.B. Tibiriçá, Heat transfer coefficient: a review of measurement techniques, *Journal of the Brazilian Society of Mechanical Sciences and Engineering*, 41 (2019) 264.
- [6] S. Han, R.J. Goldstein, The heat/mass transfer analogy for a simulated turbine endwall, *Int. J. Heat Mass Transfer*, 51 (2008) 3227-3244.
- [7] M.-S. Chae, D.-Y. Lee, B.-J. Chung, Experimental study on local variation of buoyancy-aided mixed convection heat transfer in a vertical pipe using a mass transfer method, *Exp. Therm Fluid Sci.*, 104 (2019) 105-115.
- [8] D.N.N. Duarte, DIRECT TEMPERATURE GRADIENT MEASUREMENT USING INTERFEROMETRY, *Experimental Heat Transfer*, 12 (1999) 279-294.
- [9] S. Bahl, J.A. Liburdy, Measurement of local convective heat transfer coefficients using three-dimensional interferometry, *Int. J. Heat Mass Transfer*, 34 (1991) 949-960.
- [10] S.A. Putnam, S.B. Fairchild, A.A. Arends, A.M. Urbas, All-optical beam deflection method for simultaneous thermal conductivity and thermo-optic coefficient ( $dn/dT$ ) measurements, *J. Appl. Phys.*, 119 (2016) 173102.
- [11] M. Mehrvand, S.A. Putnam, Probing the Local Heat Transfer Coefficient of Water-Cooled Microchannels Using Time-Domain Thermoreflectance, *J. Heat Transfer*, 139 (2017) 112403.
- [12] R.J. Murdock, S.A. Putnam, S. Das, A. Gupta, E.D. Chase, S. Seal, High-Throughput, Protein-

Targeted Biomolecular Detection Using Frequency-Domain Faraday Rotation Spectroscopy, *Small*, 13 (2017).

[13] T. Germain, T.A. Chowdhury, J. Carter, S.A. Putnam, Measuring Heat Transfer Coefficients for Microchannel Jet Impingement Using Time-domain Thermoreflectance, 2018 17th IEEE Intersociety Conference on Thermal and Thermomechanical Phenomena in Electronic Systems (ITherm), 2018, pp. 449-454.

[14] M. Mehrvand, S.A. Putnam, Transient and local two-phase heat transport at macro-scales to nano-scales, *Communications Physics*, 1 (2018) 21.

[15] T. Chen, S. Song, Y. Shen, K. Zhang, P. Jiang, Simultaneous measurement of thermal conductivity and heat capacity across diverse materials using the square-pulsed source (SPS) technique, *International Communications in Heat and Mass Transfer*, 158 (2024) 107849.

[16] T. Chen, S. Song, R. Hu, P. Jiang, Comprehensive measurement of three-dimensional thermal conductivity tensor using a beam-offset square-pulsed source (BO-SPS) approach, *International Journal of Thermal Sciences*, 207 (2025) 109347.

[17] M.J. Assael, K.D. Antoniadis, J. Wu, New Measurements of the Thermal Conductivity of PMMA, BK7, and Pyrex 7740 up to 450K, *International Journal of Thermophysics*, 29 (2008) 1257-1266.

[18] L. Huang, M.S. El-Genk, Heat transfer of an impinging jet on a flat surface, *Int. J. Heat Mass Transfer*, 37 (1994) 1915-1923.

[19] H. Martin, Heat and mass transfer between impinging gas jets and solid surfaces, *Advances in heat transfer*, Elsevier 1977, pp. 1-60.